



# Low-noise Yb:CALGO optical frequency comb

LISA M. MOLteni,<sup>1,2</sup>  FRANCESCO CANELLA,<sup>1</sup>  FEDERICO PIRZIO,<sup>3</sup>  MARKUS BETZ,<sup>4</sup> EDOARDO VICENTINI,<sup>2</sup>  NICOLA COLUCCELLI,<sup>1,2</sup>  GIULIANO PICCINNO,<sup>5</sup> ANTONIANGELO AGNESI,<sup>3</sup> PAOLO LAPORTA,<sup>1,2</sup> AND GIANLUCA GALZERANO<sup>1,2,\*</sup> 

<sup>1</sup>*Dipartimento di Fisica, Politecnico di Milano, Piazza Leonardo da Vinci 32, 20133 Milano, Italy*

<sup>2</sup>*Istituto di Fotonica e Nanotecnologie - CNR, Piazza Leonardo da Vinci 32, 20133 Milano, Italy*

<sup>3</sup>*Dipartimento di Ingegneria Industriale e dell'Informazione, Università Pavia, Via Ferrata 5, 27100 Pavia, Italy*

<sup>4</sup>*Technische Universität Dortmund, Otto-Hahn-Str. 4, D- 44221 Dortmund, Germany*

<sup>5</sup>*Bright Solutions SRL, Via degli Artigiani 27, 27010 Cura Carpignano (PV), Italy*

\*[gianluca.galzerano@polimi.it](mailto:gianluca.galzerano@polimi.it)

**Abstract:** We report on a compact optical frequency comb, operating in the wavelength range from 670 to 1500 nm, based on diode-pumped low-noise femtosecond Yb:CALGO amplified laser system. Both the carrier-envelope offset and repetition rate are phase-locked to reference synthesizers. A full characterization of the frequency comb, in terms of frequency stability, phase noise analysis, and optical beating against a single-frequency non-planar ring oscillator Nd:YAG laser, is presented, showing the excellent properties of the Yb:CALGO comb.

© 2021 Optical Society of America under the terms of the [OSA Open Access Publishing Agreement](#)

## 1. Introduction

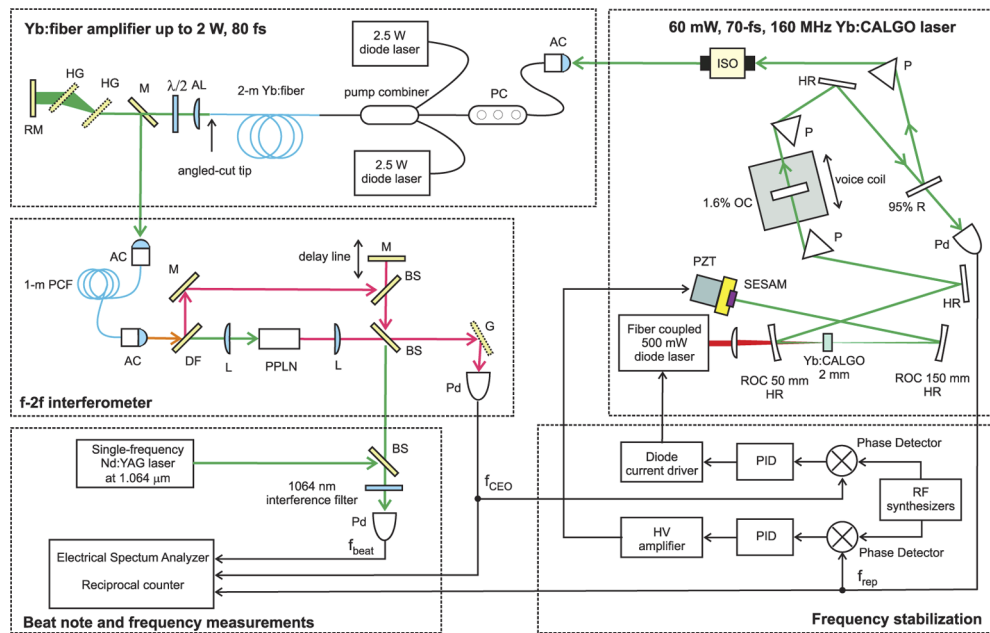
Thanks to their unique properties, optical frequency combs, originally developed in the 1999 for optical frequency metrology [1,2], have found innumerable applications over the past decade ranging from fundamental physics to astronomy, from broadband spectroscopy to environmental and biological sciences as well as from quantum optics sensing to microscopy and hyper-spectral imaging [3]. Even today, several research groups and high-tech companies are strongly interested in developing compact and very low-noise comb sources with scalable output power up to 10 W and flexible selection of the frequency comb spacing. Among the different technological implementations [3–5], solid-state laser combs are still demonstrating excellent performance with high flexibility of comb repetition rate, power scalability, and compactness similar to that of the more common fiber combs [6–8]. In particular, frequency combs based on Yb-doped crystals with emission in the 1- $\mu$ m range have become fairly popular in the last five years and have been the subject of several studies and developments [9].

In this paper, we report on a fully stabilized Yb:CaGdAlO<sub>4</sub> (Yb:CALGO) frequency comb operating in the wavelength spectral region from 670 to 1500 nm showing low-noise phase performance combined to power scalability up to watt level or even higher. The comb is based on a master-oscillator power-amplifier configuration to enhance the low-noise performance. The master oscillator is a low-power semiconductor saturable absorber mirror (SESAM) mode-locked Yb:CALGO laser at 160-MHz repetition frequency pumped by a single-mode diode laser whereas optical amplification is achieved by a diode-pumped Yb: fiber amplifier. Low-power Yb:CALGO mode-locked lasers were proved to be simple and effective sources for generating pulses as short as 36 fs using SESAMs [10] and even shorter and more powerful pulse trains by adopting Kerr-lens mode-locking (KLM) [11]. Self-referenced stabilization of a diode-pumped Yb:CALGO laser was first demonstrated with a pulse repetition rate of 1 GHz [12]. However, the large linewidth of the free-running carrier envelope offset frequency (CEO) up to several hundred of kilohertz (full width at half maximum, FWHM), mainly due to the adopted multi-transverse-mode pump diode

[12,13], made its stabilization more challenging and resulted in optical comb linewidth of  $\sim 300$  kHz for 1-ms observation times [13]. Even the different implementations of the commonly used Yb:fiber comb technology [14–16] have demonstrated free-running CEO linewidths typically ranging from 3 MHz to 150 kHz. A narrower CEO linewidth of  $\sim 10$  kHz has been recently obtained operating the mode-locked Yb:fiber laser far away from the spontaneous emission peak and with close to zero intracavity group velocity dispersion [16]. Here, we demonstrated a free-running CEO linewidth as narrow as 1.6 kHz and a comb optical linewidth narrower than 28 kHz in 1-ms observation time at 1064 nm. The whole characterization of the combs is presented by measuring the power spectral densities of both intensity and phase noises as well as the comb frequency stability in the time domain and the optical beat note against a narrow emission linewidth Nd:YAG non-planar-ring-oscillator laser at 1064 nm.

## 2. Yb:CALGO laser frequency comb

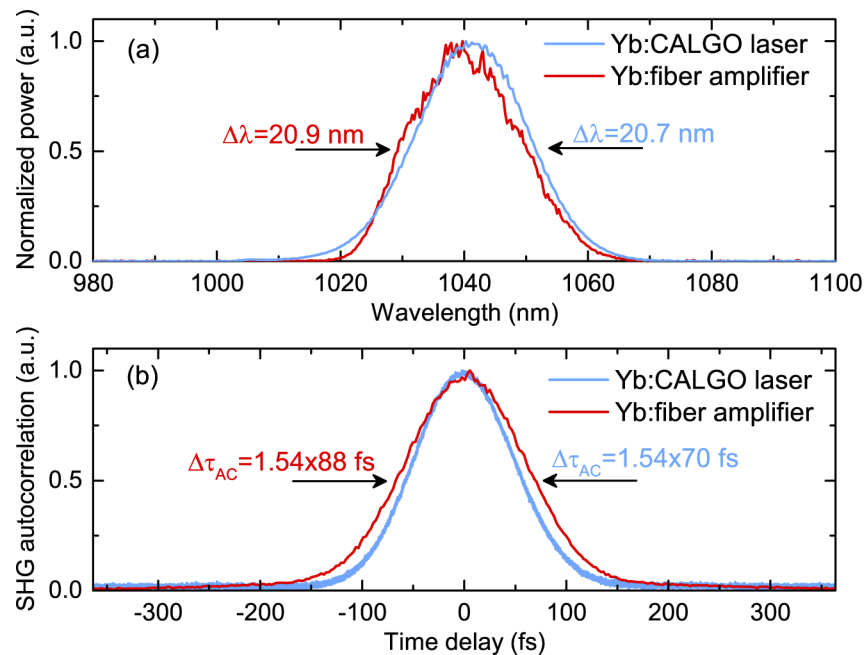
A complete scheme of the Yb:CALGO frequency comb and of its experimental characterization is shown in Fig. 1. A compact SESAM mode-locked Yb:CALGO oscillator generates pulse trains with maximum average power of 60 mW, pulse duration of 70 fs, and repetition frequency of 160 MHz. The self-starting mode-locked laser, based on a previously reported design [10], is constituted by a 2-mm thick 5%-at Yb:CALGO crystal (*a*-cut) pumped along the  $\pi$ -polarization by a fiber Bragg-grating-stabilized diode laser (Lumics, SN0958003) delivering a maximum output power of 500 mW at a central wavelength of 976 nm out of a single-mode fiber (HI 1060 fiber). The X-folded laser resonator consists of a dichroic curved mirror with a radius of



**Fig. 1.** Yb:CALGO optical frequency comb and frequency characterization experimental setup. AL: aspheric lens; AC: aspheric collimator; BS: beam splitter; DF: dichroic filter; G: reflecting grating; HG: transmitting holographic grating; HR: high-reflectivity dielectric mirror; ISO: optical isolator; L: lens; M: mirror; OC: output coupler; P: fused silica prism; PC: fiber polarization controller; PCF: photonics crystal fiber; Pd: fast photodetector; PPLN: periodically-poled lithium niobate crystal; PID: proportional-integrative-derivative servo; PZT: piezoelectric transducer; RM: roof mirror.

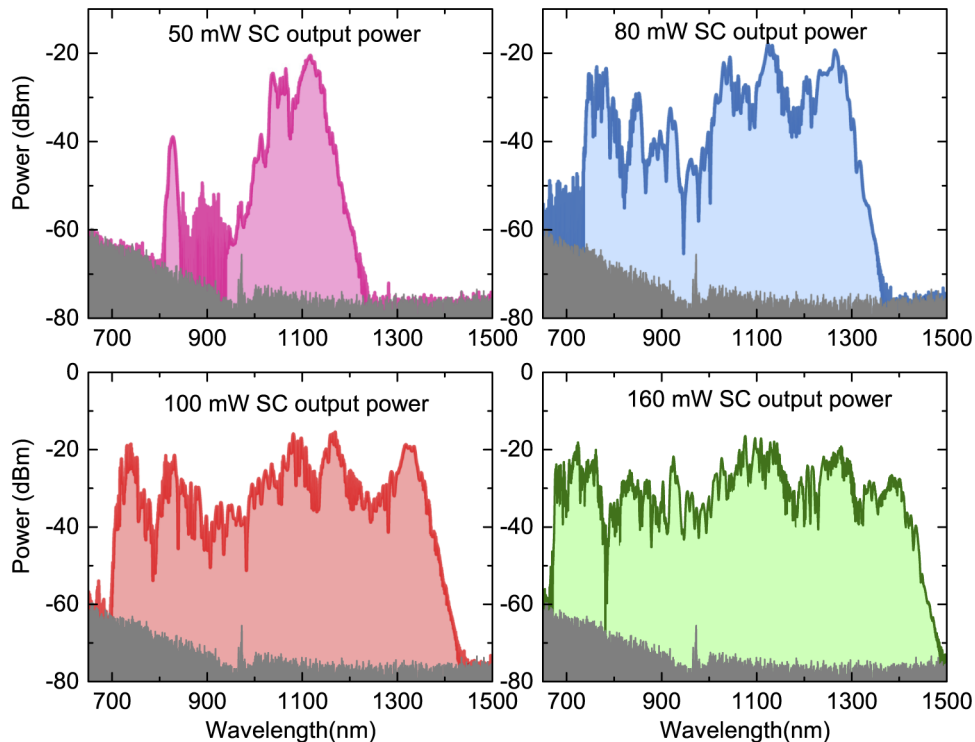
curvature (ROC) of 50 mm (highly transmitting at the pump wavelength and highly reflective at the lasing wavelength), a high-reflectivity (HR) 150-mm ROC curved mirror, a SESAM, a HR plane folding mirror, and an output coupler (OC) with 1.6% transmission. The SESAM, with a modulation depth of 3%, nonsaturable loss less than 1%, and a saturation fluence of  $140 \mu\text{J}/\text{cm}^2$ , is mounted on a piezoelectric transducer (PZT) driven by a high-voltage amplifier (HVA) for fine cavity length control (stabilization of the pulse repetition frequency). In order to minimize the cavity mode astigmatism in the active medium (calculated beam radius at the crystal of  $18 \mu\text{m}$ ), the resonator curved mirror folding angles were kept as small as possible. For intracavity Group Delay Dispersion (GDD) management, we implemented a single fused-silica prism configuration [17]. The OC is mounted on a linear stage with a large stroke of 20 mm, which turns out in a coarse tuning of both the pulse repetition and carrier envelope offset frequencies.

Figure 2 shows the spectrum (panel a) and intensity autocorrelation (panel b) of the soliton mode-locked pulse train at 60 mW average power. A nearly transform limited hyperbolic secant pulses with a duration of 70 fs and a spectrum of 20.7 nm centered at around 1041 nm are generated at a pulse repetition frequency of 160 MHz (corresponding to a pulse peak power of  $\sim 5 \text{ kW}$ ). To further increase the pulse peak power for efficient generation of an octave spanning supercontinuum (SC), the Yb:CALGO laser is coupled through an optical isolator to a low-noise Yb-doped fiber amplifier. The amplifier is constituted by 1.8-m long large mode area, polarization maintaining, Yb-doped fiber with a core diameter of  $10 \mu\text{m}$  (Liekki YB1200-10/125DC-PM). The active fiber is cladding pumped by two fiber-coupled diode lasers, each emitting 2.5 W at 976 nm in a  $50 \mu\text{m}$  core diameter, using a (2+1)x1 pump and signal combiner. The polarization of the injected pulses is adjusted by a compact in-line fiber optic polarization controller. The active fiber tip at the amplifier output is cut with an angle of  $8^\circ$  to prevent parasitic laser action in the high-gain Yb amplifier. The amplifier output beam is collimated by an aspherical lens (focal



**Fig. 2.** (a) Optical spectrum and (b) pulse intensity autocorrelation of the Yb:CALGO mode-locked laser (average power 60 mW) and of the Yb:fiber amplifier (average power 1 W).  $\Delta\lambda$  and  $\Delta\tau_{AC}$  represent the full width at half maximum values of the pulse spectrum and intensity autocorrelation traces, respectively.

length of 11 mm) and passes through a half-wave plate to control the polarization before the pulse compressor stage. The pulse compressor is constituted by a pair of transmission gratings, 800 grooves/mm (Wasatch Photonics), placed at a distance of  $\sim 2.0$  cm and at an incidence angle of  $24^\circ$ , and a roof aluminium mirror. The total efficiency of the compressor is 55%. The maximum power at the compressor output is 1 W with a minimum pulse duration of  $\sim 90$  fs, corresponding to a maximum peak power of  $\sim 70$  kW. The spectrum and intensity autocorrelation of the amplified pulse trains are shown in Fig. 2. The amplified pulses are then coupled with a 50% efficiency into a 1-m long photonic crystal fiber (PCF) with a zero dispersion wavelength of 975 nm for SC spectrum generation (NKT-SC-3.7-975). For a power of 160 mW at the output of the PCF the SC spectrum covers a full frequency octave ranging from 650 nm to 1500 nm at  $-30$  dB from the maximum power achieved at  $\sim 1400$  nm, as shown in Fig. 3. An excellent long-term stability of the PCF coupling efficiency and of the generated SC spectra is obtained by equipping the PCF fiber with standard FC-APC connectors and connectorized high NA collimators. Even broader SC spectra can be obtained increasing the input pump power but the best signal-to-noise ratio (SNR) for the detection of the carrier envelope offset (CEO) frequency was obtained for 160 mW SC power. The SC radiation is then sent into a traditional  $f$ -to- $2f$  interferometer (see Fig. 1) for the detection of CEO frequency. The SC spectrum is separated at the input of the  $f$ -to- $2f$  interferometer by using a low-pass dichroic filter with a cut-off wavelength of  $\sim 1000$  nm into short ( $< 1000$  nm) and long ( $> 1000$  nm) wavelength components, respectively. The two beams propagate along two different optical paths: the long wavelength component is focused on a 10-mm long periodically-poled lithium niobate crystal for quasi-phase matched second harmonic generation at 700 nm ( $15.1 \mu\text{m}$  poling period), whereas the short wavelength component passes



**Fig. 3.** SC spectra at the output of the PCF for different output power levels recorded with a resolution bandwidth of 0.1 nm. Gray curve represents the instrument noise floor (Ando AQ6317C).

through an adjustable delay line. The two components are then combined using a beam splitter, filtered with a reflection grating at around 700 nm, and detected by a fast Si-photodiode. In addition, the long wavelength component is also combined with a single-frequency Nd:YAG laser operating at 1064 nm with a free-running emission linewidth of  $\sim 10$  kHz for 1-ms observation times, for a direct characterization of the Yb:CALGO frequency comb by means of the optical heterodyne beatnote.

### 3. Results

#### 3.1. Relative intensity noise

The relative intensity noise (RIN) characterization of the Yb:CALGO frequency comb is performed on the SC radiation as well as on the Yb:CALGO mode-locked laser and Yb-fiber amplifier. In the case of the SC radiation, RIN measurements are obtained after a proper optical filtering (based on a reflection grating in a  $2f$  configuration allowing for a bandwidth of  $\sim 10$  nm) and by using a low-noise Si photodetector for wavelengths shorter than 1100 nm and a low-noise InGaAs photodetector for longer wavelengths. Figure 4 summarizes the measured RIN spectra in the Fourier frequency range from 1 Hz to 80 MHz (Nyquist frequency). In the low-frequency Fourier range the Yb:CALGO mode-locked laser is characterized by a RIN spectrum equivalent to that of its single-transverse-mode pump diode, which is mainly limited by a flicker noise contribution. For higher Fourier frequencies, the Yb:CALGO RIN spectrum is always lower than the pump diode due to a filtering effect of the Yb upper laser level lifetime (440  $\mu$ s, corresponding to a cut-off frequency of  $\sim 360$  Hz), and for frequencies larger than 10 kHz the power spectral density of the RIN reaches the noise-floor at the level of -123 dB/Hz. A similar behavior is also observed for the fiber amplified pulse trains, apart some extra noise at the line frequency and its harmonics up to 900 Hz, due to the current noise of the high-power fiber-amplifier pump diode drivers. Over the frequency range from 10 Hz to 80 MHz the cumulative standard deviation of the Yb:CALGO laser and Yb:fiber amplified pulses amount, respectively, to 0.21% and 0.20%. Compared to the input amplified pump radiation, the RIN of the SC is mainly degraded in the low Fourier frequencies range from 1 Hz to 10-100 kHz, whereas the degradation of the white noise floor in the high-frequency region, due to the nonlinear amplification of the input-pulse shot noise [18], is less than 6 dB with respect to the amplified pulse noise. The low-frequency behavior of the SC RIN spectra is ascribed to modulation instability of the higher-order soliton propagation dynamics compared to the 1-m long PCF [19,20]. In particular, the main RIN degradation is observed for the Raman frequency shifted soliton at around 1400 nm. Over the frequency range from 10 Hz to 80 MHz the cumulative standard deviation of the SC at the PCF output amounts to 0.31% (at 700 nm), 0.47% (at 1000 nm), and 1.07% (at 1400 nm).

#### 3.2. Carrier-envelope-offset frequency and comb stabilization

Figure 5(a) shows the CEO beat note recorded at the output of the  $f$ -to- $2f$  interferometer with a SNR of  $\sim 35$  dB in a resolution bandwidth of 25 kHz. It is worth noting that in free-running regime the CEO frequency is characterized by a linewidth as narrow as 1.6 kHz (instrument limited) and a SNR as large as 47 dB, as reported in the inset of Fig. 5(b), a clear evidence of the low-noise properties of the Yb:CALGO fiber-amplified comb. This behaviour is ascribed to different technological implementations: i) the use of a high-quality factor Yb:CALGO laser resonator with low intracavity losses to reduce the quantum noise (spontaneous emission) contribution [21]; ii) the adoption of a single-transverse-mode diode laser to pump the Yb:CALGO laser with low intensity noise [22,23]; an overall good isolation against environmental perturbations such vibrations and temperature fluctuations [22,23]. The whole characterization of the CEO and comb repetition frequencies is realized both in frequency and time domains using, respectively, an electrical spectrum analyzer to measure the phase-noise power spectral densities and a

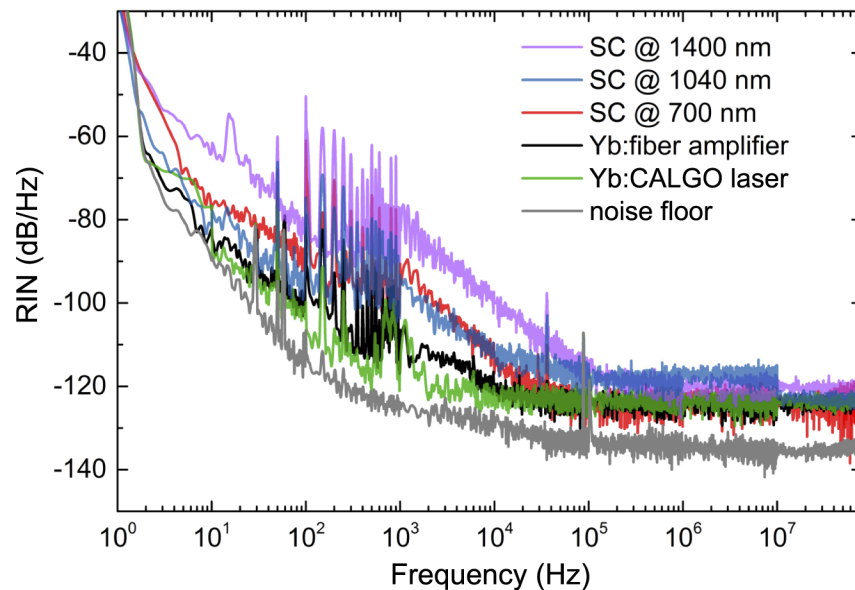


**Fig. 4.** Relative intensity noise spectra of the SC at different wavelength regions together with the relative intensity noise of the Yb: fiber amplifier and Yb: CALGO laser.

reciprocal electronic counter to record the average frequencies versus integration times. This characterization is performed both in free-running and frequency stabilized regimes. Indeed, CEO and repetition rate frequencies have been actively stabilized against RF synthesizers, referenced to a rubidium RF standard (fractional frequency accuracy of  $10^{-12}$ ), using two opto-electronics phase-locked-loop (PLL) schemes acting on the Yb: CALGO pump diode for CEO stabilization and on the Yb: CALGO cavity length for the stabilization of the repetition frequency. In particular, the CEO beatnote is compared to a RF synthesizer in a low-noise phase detector, whose output error signal is sent to a proportional integral derivative (PID) servo acting on the pump diode current driver (see Fig. 1). The measured transfer function between the CEO frequency and the diode current behaves like a damped pair of complex conjugated poles with a resonance cut-off frequency of 35 kHz (phase  $90^\circ$ ), in good agreement with the theoretical prediction of the relaxation oscillation of our mode-locked cavity dynamics [24]. In the case of repetition rate stabilization, to further increase the sensitivity, the fourth harmonic of the repetition frequency at around  $\sim 640$  MHz is compared to the RF synthesizer into a doubled-balanced mixer acting as phase detector. Also in this case, the error signal at the output of the doubled-balanced mixer is sent to a PID servo supplying the high-voltage amplifier that drives the PZT actuator for active control of the Yb: CALGO resonator length with a maximum bandwidth of 5 kHz, limited by the mechanical PZT resonances.

Figure 6 shows the phase-noise power spectral densities in the free-running and locked regimes of the CEO frequency (panel a) and of the repetition frequency (panel b), respectively, in the Fourier frequency range from 10 Hz to 1 MHz. A phase-locking bandwidth of  $\sim 30$  kHz is assessed from the position of the crossing point between the free-running (blue curve) and the locked (red curve) phase-noise power spectral densities. This control loop bandwidth is limited by the presence in the transfer function of CEO frequency with respect to the pump diode current of the pair of complex conjugated poles that can not be compensated by the adopted PID servo. However, thanks to the narrow free-running CEO linewidth, as narrow as 1.6 kHz, this control bandwidth is large enough to show a coherent peak in the CEO beat note. For Fourier frequencies higher than 40 kHz the recorded phase-noise spectral densities are mainly limited by the finite

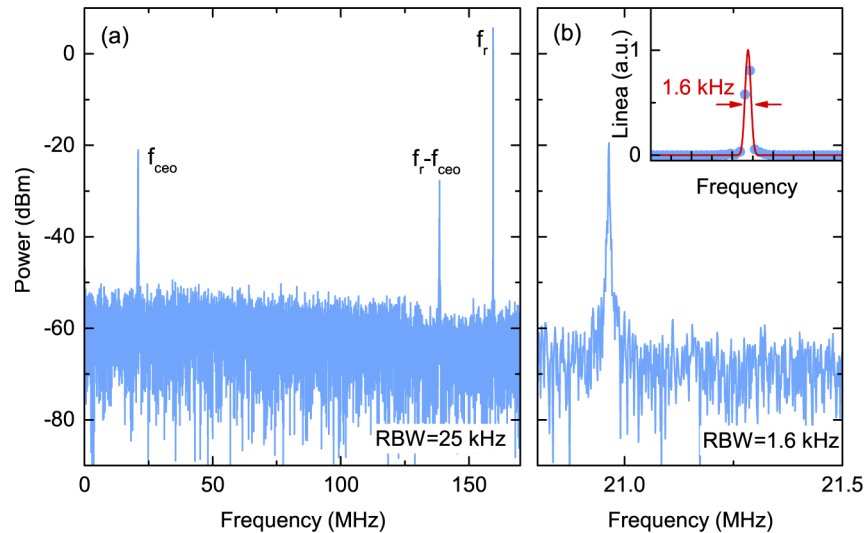


**Fig. 5.** (a) RF spectrum of the signal at the output of the  $f$ -to- $2f$  interferometer showing the beat note at the CEO frequency of  $\sim 21$  MHz with a SNR of higher than 30 dB in 25 kHz resolution bandwidth. (b) Detailed spectrum of the CEO beatnote frequency with 700-kHz frequency span and 1.6-kHz resolution bandwidth, showing a SNR of 47 dB and a full width at half maximum linewidth limited by the adopted resolution bandwidth (see inset in linear scale: red curve is a Gaussian fitting curve with 1.6 kHz linewidth).

SNR of the CEO beatnote. In phase-locking condition the integrated phase noise of the CEO signal is 0.34 rad in the bandwidth from 10 to 1 MHz. In the case of repetition frequency, the stabilization control loop bandwidth is set to approximately 400 Hz, as shown in Fig. 6(b), to avoid excess multiplication of the synthesizer phase noise in the optical domain. To validate the frequency stability of the self-referenced Yb:CALGO comb in the time domain, the CEO and repetition rate frequencies are directly measured by using a reciprocal electronic counter (referenced to the same Rb clock).

Figure 7 shows sequential time series of the measured repetition rate (panel a) and CEO frequency (panel b) with a counter gate time of 0.1 s for different locking conditions. In free-running condition the stability of the comb is mainly limited by the thermal drift of the cavity length, reflecting on a drift of 0.5 Hz/s in the pulse repetition rate, which corresponds to a thermal drift of the aluminium laser breadboard of 0.13 mK/s and a frequency drift of the optical carrier of 1 MHz/s (assuming 300 THz for the optical carrier at around  $1 \mu\text{m}$ ). By the simultaneous measurement of the drifts in the repetition rate and CEO frequencies in free-running conditions, we also retrieved the ratio between the intracavity group and phase velocities, using the simple relation  $f_{CEO} = \nu_c(1 - \nu_g/\nu_p)$ , where  $\nu_c$  is the carrier frequency,  $\nu_g$  and  $\nu_p$  are, respectively, the group and phase velocity inside the Yb:CALGO mode-locked laser [25]. From the data reported in Fig. 7 (free-running conditions) a  $\nu_g/\nu_p$  of 0.988 is obtained. When the repetition frequency is stabilized against the RF synthesizer, a strong reduction of the frequency drift from 12 kHz/s down to 1 kHz/s is observed for the free-running CEO signal (green curve in Fig. 7(b)). This residual drift is ascribed to thermal fluctuations in the Yb:CALGO crystal and in the aluminium breadboard, acting on the intracavity group delay dispersion compensation. The stabilization of the CEO frequency allows the full referencing of the Yb:CALGO comb. To better understand the long-term stability of the realized Yb:CALGO comb, we computed the overlapping Allan deviation,  $\sigma_y(\tau)$  where  $\tau$  is the integration time, from the full-locking condition time series reported in Fig. 7 (red curves). Figure 8 shows the contribution of the CEO and repetition

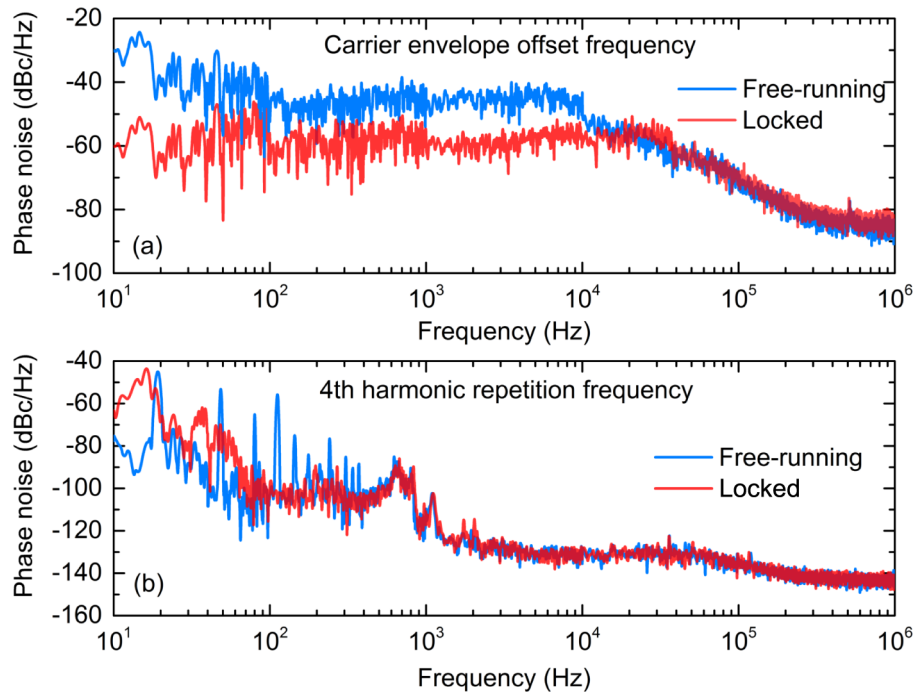


**Fig. 6.** Phase-noise power spectral density of the (a) carrier envelope offset and (b) 4-th harmonics of the comb repetition frequencies, when the Yb:CALGO frequency comb is in free-running (blue curves) and frequency stabilized against RF reference (red curves).

frequency to the long-term stability of the Yb:CALGO. It is worth noting that the contribution of the stabilized CEO, characterized by a white frequency noise law,  $\sigma_y(\tau) = 5 \times 10^{-14} \cdot \tau^{-1/2}$ , is more than two orders of magnitude lower than the measured repetition frequency stability and reaches the  $7 \times 10^{-15}$  level at 100-s integration time. By an optimized servo-loop electronics the long-term stability of the stabilized CEO frequency would be further improved, following a white phase noise contribution corresponding to  $\tau^{-1}$  dependence of the CEO Allan deviation [26,27]. The contribution of the repetition frequency stability, at the level of  $\sigma_y(\tau) = 6 \times 10^{-12} \cdot \tau^{-1/2}$ , is somewhat part limited by the finite resolution of the adopted electronic counter (dashed black curve in black dot in Fig. 8). For integration times as long as 100 s, the overall fractional stability of the Yb:CALGO comb is at a level of  $7 \times 10^{-13}$ , which corresponds to the stability of the Rb reference clock.

Finally, a heterodyne beatnote between the frequency-stabilized Yb:CALGO comb and a free-running single-frequency Nd:YAG non-planar-ring-oscillator is detected to directly measure the linewidth of the optical comb tooth at around 1064 nm. Figure 9 reports the RF spectrum of the beatnote signal showing a SNR of 25 dB in a resolution bandwidth of 20 kHz. The beatnote signal is characterized by a full-width at half-maximum linewidth of 28 kHz when recorded with a resolution bandwidth of 9 kHz (0.1 ms integration time), which turns out to be the linewidth of the comb tooth being the contribution of the Nd:YAG linewidth negligible (of the order of 1-kHz) for integration times of 0.1 ms. The low-noise properties of the Yb:CALGO comb, as highlighted by extremely narrow linewidths of both the carrier envelope offset frequency (1.6 kHz) and the comb tooth (28 kHz), have been mainly ascribed by the adoption of a low-noise single-transverse-mode pump diode laser and a high-Q Yb:CALGO laser resonator combined to an overall good isolation against environmental perturbations.

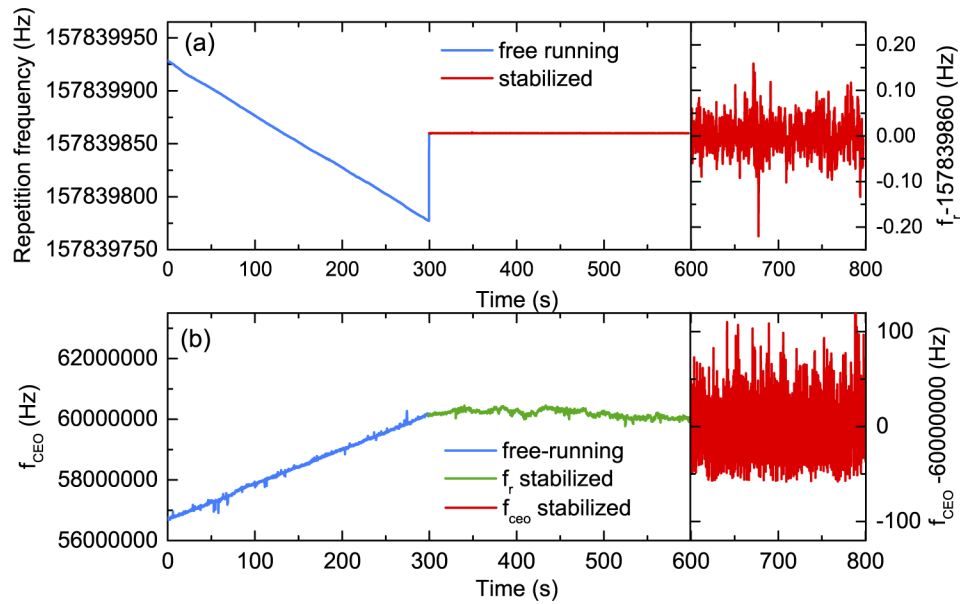


**Fig. 7.** Time domain stability of (a) repetition and (b) CEO frequencies as recorded by the electronic counter with 100 ms gate time. Right vertical axes refer to stabilized regimes.

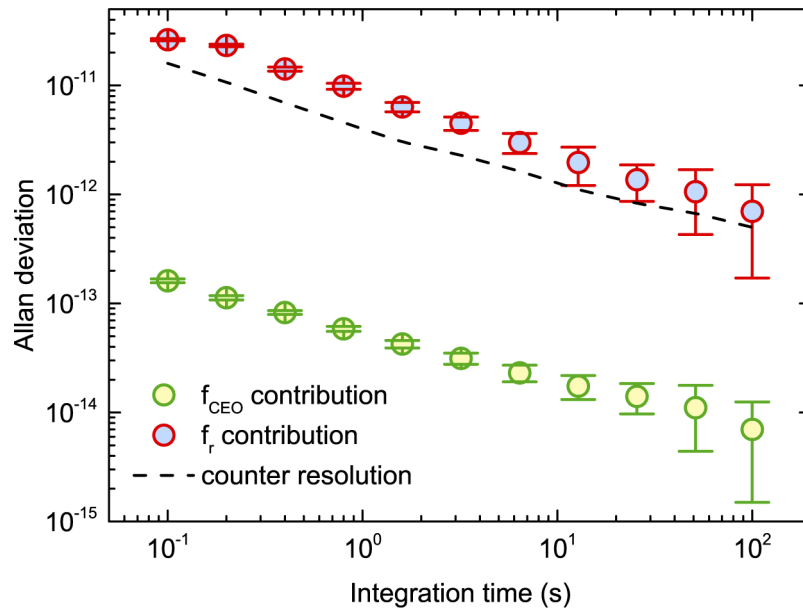


**Fig. 8.** Computed overlapped Allan deviation from the measurements reported in Fig. 7 versus integration time when the Yb:CALGO comb is stabilized against RF reference. Dashed line represents the electronic counter fractional frequency resolution.

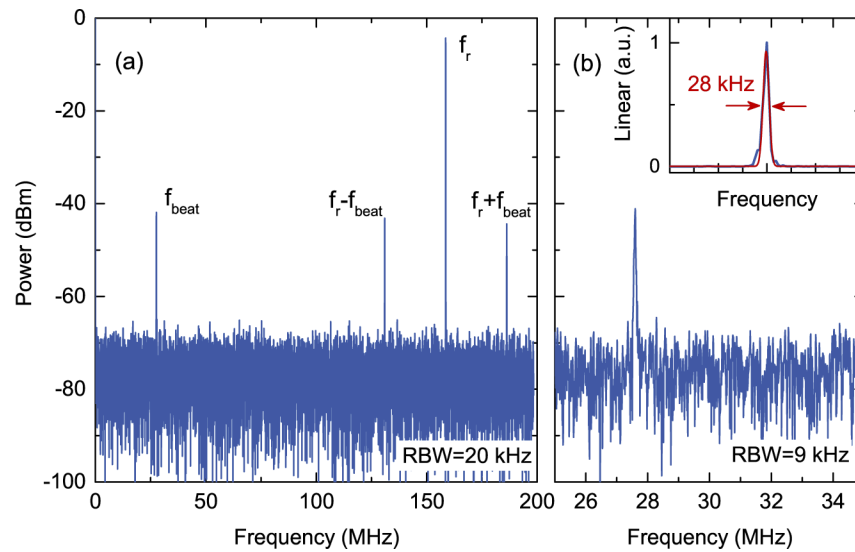


**Fig. 9.** (a) RF spectrum of the beat note signal between the Yb:CALGO comb and the narrow-linewidth Nd:YAG laser showing a SNR of higher than 25 dB in 20 kHz resolution bandwidth. (b) Detailed spectrum of the beatnote signal with 9-kHz resolution bandwidth, showing a SNR of 31 dB and a full width at half maximum linewidth of 28 kHz (see inset in linear scale: red curve is a Gaussian fitting curve).

#### 4. Conclusion

We reported on a self-referenced frequency comb based on a compact Yb:CALGO ultrafast laser system covering the spectral range from 650 to 1500 nm. The whole characterization in the frequency and time domains demonstrated the excellent properties of the proposed optical frequency comb making a versatile tool in frequency metrology and high-resolution spectroscopy. The long-term relative frequency stability of the comb was limited at the level of  $7 \times 10^{-13}$  (at 100-s averaging time) by the reference synthesizer used in the repetition rate stabilization, whereas the frequency instability of the locked carrier envelope offset frequency contributed only at the level of  $7 \times 10^{-15}$ . Further improvement of the long term stability can be achieved by using a better RF reference signal, such as hydrogen maser, or alternatively by adopting an optical reference to lock the comb repetition frequency.

**Disclosures.** The authors declare no conflicts of interest.

**Data availability.** Data underlying the results presented in this paper are not publicly available at this time but may be obtained from the authors upon reasonable request.

#### References

1. T. Udem, J. Reichert, R. Holzwarth, and T. W. Hänsch, "Absolute optical frequency measurement of the cesium  $d_1$  line with a mode-locked laser," *Phys. Rev. Lett.* **82**(18), 3568–3571 (1999).
2. D. J. Jones, S. A. Diddams, J. K. Ranka, A. Stentz, R. S. Windeler, J. L. Hall, and S. T. Cundiff, "Carrier-envelope phase control of femtosecond mode-locked lasers and direct optical frequency synthesis," *Science* **288**(5466), 635–639 (2000).
3. T. Fortier and E. Baumann, "20 years of developments in optical frequency comb technology and applications," *Commun. Phys.* **2**(1), 153 (2019).
4. S. A. Diddams, "The evolving optical frequency comb invited," *J. Opt. Soc. Am. B* **27**(11), B51–B62 (2010).
5. A. Schliesser, N. Picqué, and T. W. Hänsch, "Mid-infrared frequency combs," *Nat. Photonics* **6**(7), 440–449 (2012).
6. A. Ruehl, "Advances in yb:fiber frequency comb technology," *Opt. Photonics News* **23**(5), 30–35 (2012).
7. N. Kuse, J. Jiang, C. C. Lee, T. R. Schibli, and M. E. Fermann, "All polarization-maintaining fiber-based optical frequency combs with nonlinear amplifying loop mirror," *Opt. Express* **24**(3), 3095–3102 (2016).

8. W. Hänsel, H. Hoogland, M. Giunta, S. Schmid, T. Steinmetz, R. Doubek, P. Mayer, S. Dobner, C. Cleff, M. Fischer, and R. Holzwarth, "All polarization-maintaining fiber laser architecture for robust femtosecond pulse generation," *Appl. Phys. B* **123**(1), 41 (2017).
9. S. Schilt and T. Südmeyer, "Carrier-envelope offset stabilized ultrafast diode-pumped solid-state lasers," *Appl. Sci.* **5**(4), 787–816 (2015).
10. F. Pirzio, M. Kemnitzer, A. Guandalini, F. Kienle, S. Veronesi, M. Tonelli, J. Aus der Au, and A. Agnesi, "Ultrafast, solid-state oscillators based on broadband, multisite yb-doped crystals," *Opt. Express* **24**(11), 11782–11792 (2016).
11. P. Sévillano, P. Georges, F. Druon, D. Descamps, and E. Cormier, "32-fs kerr-lens mode-locked yb:cagdalo4 oscillator optically pumped by a bright fiber laser," *Opt. Lett.* **39**(20), 6001–6004 (2014).
12. A. Klenner, S. Schilt, T. Südmeyer, and U. Keller, "Gigahertz frequency comb from a diode-pumped solid-state laser," *Opt. Express* **22**(25), 31008–31019 (2014).
13. S. Hakobyan, V. J. Wittwer, P. Brochard, K. Gürel, S. Schilt, A. S. Mayer, U. Keller, and T. Südmeyer, "Full stabilization and characterization of an optical frequency comb from a diode-pumped solid-state laser with ghz repetition rate," *Opt. Express* **25**(17), 20437–20453 (2017).
14. P. Pal, W. H. Knox, I. Hartl, and M. E. Fermann, "Self referenced yb-fiber-laser frequency comb using a dispersion micromanaged tapered holey fiber," *Opt. Express* **15**(19), 12161–12166 (2007).
15. Y. Ma, B. Xu, H. Ishii, F. Meng, Y. Nakajima, I. Matsushima, T. R. Schibli, Z. Zhang, and K. Minoshima, "Low-noise 750-mhz spaced ytterbium fiber frequency combs," *Opt. Lett.* **43**(17), 4136–4139 (2018).
16. A. S. Mayer, W. Grosinger, J. Fellinger, G. Winkler, L. W. Perner, S. Droste, S. H. Salman, C. Li, C. M. Heyl, I. Hartl, and O. H. Heckl, "Flexible all-pm nalm yb: fiber laser design for frequency comb applications: operation regimes and their noise properties," *Opt. Express* **28**(13), 18946–18968 (2020).
17. D. Kopf, G. J. Spühler, K. J. Weingarten, and U. Keller, "Mode-locked laser cavities with a single prism for dispersion compensation," *Appl. Opt.* **35**(6), 912–915 (1996).
18. K. L. Corwin, N. R. Newbury, J. M. Dudley, S. Coen, S. A. Diddams, K. Weber, and R. S. Windeler, "Fundamental noise limitations to supercontinuum generation in microstructure fiber," *Phys. Rev. Lett.* **90**(11), 113904 (2003).
19. M. Nakazawa, K. Tamura, H. Kubota, and E. Yoshida, "Coherence degradation in the process of supercontinuum generation in an optical fiber," *Opt. Fiber Technol.* **4**(2), 215–223 (1998).
20. G. Genty, S. Coen, and J. M. Dudley, "Fiber supercontinuum sources (invited)," *J. Opt. Soc. Am. B* **24**(8), 1771–1785 (2007).
21. H. A. Haus and A. Mecozzi, "Noise of mode-locked lasers," *IEEE J. Quantum Electron.* **29**(3), 983–996 (1993).
22. R. Paschotta, A. Schlatter, S. C. Zeller, H. R. Telle, and U. Keller, "Optical phase noise and carrier-envelope offset noise of mode-locked lasers," *Appl. Phys. B* **82**(2), 265–273 (2006).
23. N. R. Newbury and W. C. Swann, "Low-noise fiber-laser frequency combs (invited)," *J. Opt. Soc. Am. B* **24**(8), 1756–1770 (2007).
24. A. Schlatter, S. C. Zeller, R. Grange, R. Paschotta, and U. Keller, "Pulse-energy dynamics of passively mode-locked solid-state lasers above the q-switching threshold," *J. Opt. Soc. Am. B* **21**(8), 1469–1478 (2004).
25. L. Matos, O. D. Mücke, J. Chen, and F. X. Kärtner, "Carrier-envelope phase dynamics and noise analysis in octave-spanning ti:sapphire lasers," *Opt. Express* **14**(6), 2497–2511 (2006).
26. Y. Nakajima, H. Inaba, K. Hosaka, K. Minoshima, A. Onae, M. Yasuda, T. Kohno, S. Kawato, T. Kobayashi, T. Katsuyama, and F.-L. Hong, "A multi-branch, fiber-based frequency comb with millihertz-level relative linewidths using an intra-cavity electro-optic modulator," *Opt. Express* **18**(2), 1667–1676 (2010).
27. K. Hitachi, K. Hara, O. Tadanaga, A. Ishizawa, T. Nishikawa, and H. Gotoh, "Reduced pulse energy for frequency comb offset stabilization with a dual-pitch periodically poled lithium niobate ridge waveguide," *Appl. Phys. Lett.* **110**(24), 241107 (2017).